PHYSICAL REVIEW D VOLUME 45, NUMBER 7 1 APRIL 1992

Intermittency and multifractality in e^+e^- annihilation

Charles B. Chiu
Center for Particle Theory and Department of Physics, University of Texas, Austin, Texas 78712

Rudolph C. Hwa
Institute of Theoretical Science and Department of Physics, University of Oregon, Eugene, Oregon 97403-5203
(Received 10 June 1991; revised manuscript received 24 October 1991)

Detailed properties of intermittency and multifractality associated with multiplicity fluctuations in e^+e^- annihilation are investigated in the framework of the Monte Carlo code JETSET for the Lund parton shower model. Dependences on energy, rapidity window width, and multiplicity are found to be very complicated. In order to extract the underlying essence of the fractal behavior, an exhaustive study is made to uncover universal properties of the intermittency indices and multifractal spectra. The latter is found to be more amenable to universal description, independent of the details of the experimental parameters.

PACS number(s): 13.65.+i, 05.45.+b, 12.40.Ee

I. INTRODUCTION

The study of self-similarity in multiplicity fluctuations has opened up a new area of investigation in multiparticle production [1]. The subject has been referred to as intermittency by Bialas and Peschanski [2], who first suggested the possibility of power-law behavior of the normalized factorial moments as functions of rapidity bin widths. The phenomenon has been observed in various collision processes involving a large variety of beam and target types [1]. Extension of that description to multifractal analysis has also been considered subsequently [3–5]. The precise connection between intermittency and multifractality has not been fully understood. Except for e^+e^- annihilation, the intermittency data have shown that the existing models on hadronic collisions are unable to account for the data [1]. In the case of e^+e^- annihilation, the Lund parton shower model [6] works very well, especially in the framework of the Monte Carlo code JETSET [7]. Yet, even in that case, only a limited aspect of intermittent behavior has been explored [8–10]. In this paper we investigate in detail a number of issues on multiplicity fluctuations in the hope of discovering universal properties that are independent of detailed experimental parameters, for it is only with the virtue of universality that one can associate fundamental significance to either the intermittency indices or the fractal dimensions.

Since the Lund shower model has been successful in giving the normalized factorial moments F_q that agree with the data of the e^+e^- annihilation experiments at the CERN e^+e^- collider LEP [8–10], we use the code JETSET to generate all the answers to questions that we pose on unexplored properties of intermittency and multifractality. Our objective will be to study the dependences on energy (squared) s, rapidity window Y, and multiplicity N in the window, which we shall refer to collectively as sYN. It is our opinion that unless the sYN dependence is fully understood, data from different experiments cannot be meaningfully compared even for collisions of the same beam-target type, let alone for different types of collisions.

As we shall show, both intermittency and multifractality have sYN dependence, a syndrome that must be fully recognized if the essence of multiplicity fluctuation is to be extracted. JETSET provides a good laboratory for us to try out various schemes of analysis. In a sense we are probing into a more central aspect of the e^+e^- annihilation problem that still awaits confrontation between theory and experiment. Moreover, it suggests that similar analysis should be carried out for other collision processes so that the universal features of the different processes can then be meaningfully compared.

II. THE sYN SYNDROME

In conventional statistical systems, the critical exponents are universal in that they are independent of the material exhibiting the critical phenomenon. In certain fractal growth phenomena, there is also an universality in the fractal dimension. To what extent are the properties of intermittency and multifractality in multiparticle production universal? Buschbeck and Lipa [11] have shown that empirically the intermittency indices generally decrease with rapidity density regardless of the colliding systems. If there is anything basic to be learned from that observation, it is necessary to understand clearly first how intermittency depends on the collision parameters even within one system. That is what we shall scrutinize for e^+e^- annihilation.

To study the sYN syndrome we shall lean on the physical reliability of JETSET to push to much higher energies than what is experimentally accessible now so that with more particles produced we can have wider ranges of variables to explore the dependencies on them. Thus, for $\sqrt{s}$ we consider 1 and 10 TeV. Values in between will not be considered, since there are too many other parameters also to vary. For Y we want it not to be so wide as to cover the extreme wings of the rapidity distribution,

dN/dy. The latter is shown in Fig. 1 for the two energies where the data are analyzed along the sphericity axis. We have chosen to consider $Y=2$ and 4 in the ranges $-1\le y\le 1$ and $-2\le y\le 2$. On N we postpone our discussion to later in this section.

Various factorial moments have been considered for intermittency studies [1,2]. For our immediate purposes here let us consider

$$F_q^{\mathrm{h,v}}\equiv\left\langle \frac{(1/M)\sum_{j=1}^{M}[n_j(n_j-1)\cdots(n_j-q+1)]}{(N/M)^q}\right\rangle , \quad (2.1)$$

where M is the total number of bins in Y, $N=\sum_{j=1}^{M}n_j$ is the total number of particles in Y for a given event, n_j is the number of particles in the jth bin in that event, and the angular brackets denote averaging over all events. We call this the normalized factorial moment obtained by "horizontal analysis, vertically averaged," abbreviated by the symbol (h,v). Note that the factorial product is normalized by (average bin multiplicity)^q, event by event, before vertical averaging. The experimental data in Refs. [8–10] are for F_q moments normalized by $(\langle N\rangle/M)^q$, where the multiplicity is averaged over all events first. The two types of F_q moments are equivalent only if N is the same for all events, which is, of course, far from reality. Equation (2.1) is closer to the moments originally suggested in Ref. [2], and is clearly more appropriate when N fluctuates strongly from event to event.

The calculated results for $F_q^{\mathrm{h,v}}$ are shown in Fig. 2 for $\sqrt{s}=1$ and 10 TeV and $Y=2$ and 4. In the figure, $\ln F_4^{\mathrm{h,v}}$ is plotted against μ, where μ is defined by

$$M=2^{\mu} . \quad (2.2)$$

A linear relationship in the $\ln F_q$ vs μ plot, or the log-log plot, would imply the power-law behavior

$$F_q\propto\delta^{-a_q} , \quad (2.3)$$

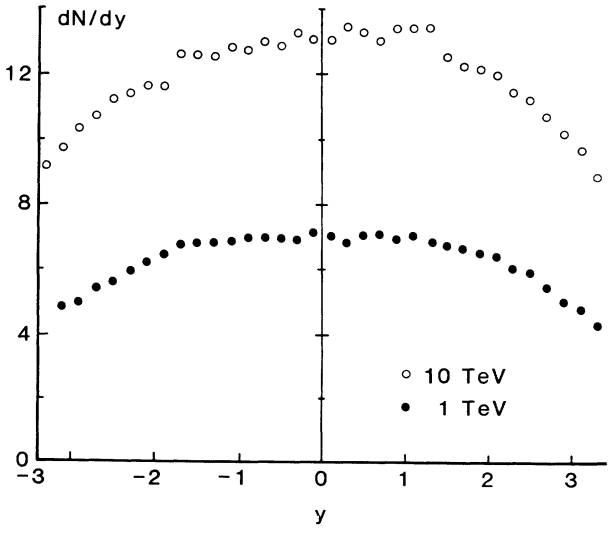

FIG. 1. Rapidity distributions at 1 and 10 TeV.

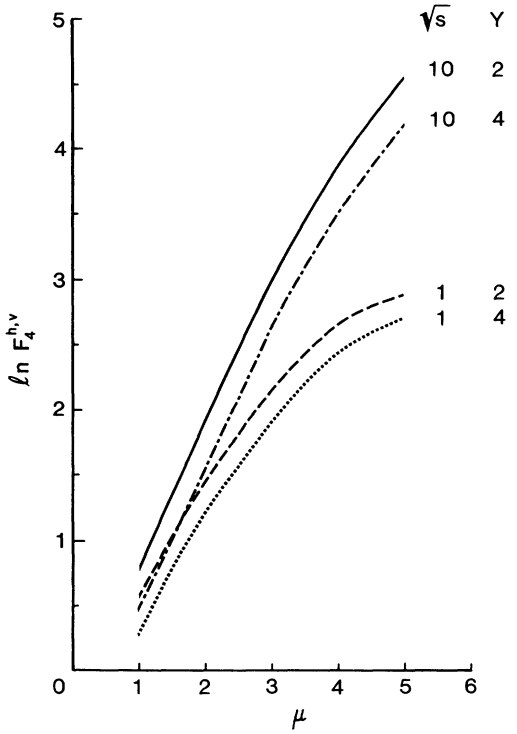

FIG. 2. log-log plot of $F_q^{\mathrm{h,v}}$ for $q=4$ and four cases of (s, Y).

where $\delta=Y/M$ and a_q is the intermittency index. Figure 2 implies that we have intermittency for all combinations of s and Y with intermittency indices a_4 (slopes of the straight-line portions in Fig. 2), that depend on s but not on Y. Similar behavior exists for other values of q also. A common consequence of increasing s and Y is that the

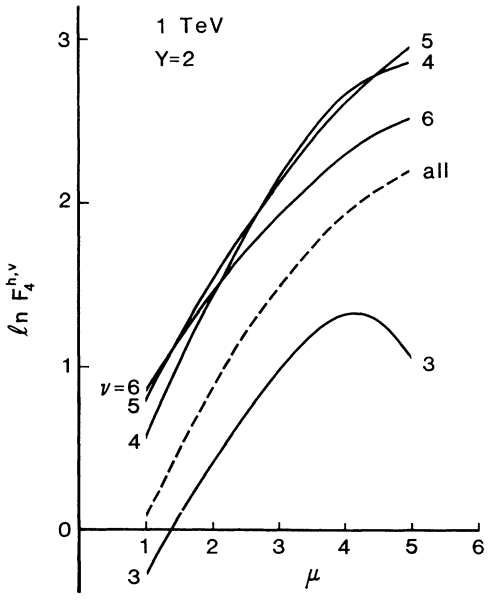

FIG. 3. log-log plot of $F_q^{\mathrm{h,v}}$ for $q=4$, $\sqrt{s}=1$ TeV, $Y=2$, and $\nu=3,\ldots,6$. The dashed line is for vertical average of F_q^{h} over all events regardless of ν (or N).

average multiplicity $\langle N \rangle$ in the window of horizontal analysis increases. Thus, it is reasonable to inquire about the dependence of $F_q^{h,v}$ on $\langle N \rangle$. However, a more incisive inquiry would be to go beyond the dependence on the average $\langle N \rangle$ and into the dependence of N itself.

We can collect all events having the same N (or in a narrow increment around N), perform averages within that sample, and then compare the results with different values of N. As a more appropriate variable we shall use ν, instead of N, where ν is defined by

$$N=2^{\nu} . \tag{2.4}$$

In Fig. 3 we show the results of our calculation for $F_4^{h,v}$ at $\sqrt{s}=1$ TeV and $Y=2$ for ν ranging from 3 to 6. We see that the slope is about the same at $\nu=4$ and 5 but it is lower at both 3 and 6. This lack of uniform behavior is found in other values of s and Y also.

With Figs. 2 and 3 we have graphically shown some signs of the sYN syndrome, a complicated pattern of dependencies that is likely to reduce the effectiveness of the intermittency analyses, unless one can discover some underlying order among the various values of a_q.

III. HORIZONTAL AND VERTICAL ANALYSES

Having seen the sYN syndrome in intermittency, we ask, on the one hand, whether it is a consequence of the particular choice of the type of analysis done, and on the other, whether the syndrome itself can be analyzed to yield some form of hidden universality. First, let us define a variant of (2.1)

$$(\ln F_q^{h})^{v} \equiv \left\langle \ln \frac{(1/M)\sum_{j=1}^{M}[n_j(n_j-1)\cdots(n_j-q+1)]}{(N/M)^q} \right\rangle , \tag{3.1}$$

where the logarithm of F_q^{h} is taken first before vertical averaging. This type of averaging makes sense if we believe that the multiplicative factor in front of δ^{-a_q} in (2.3), not shown in that equations, may fluctuate vertically to give an unwanted weight to the average of a_q. The plot $(\ln F_q^{h})^{v}$ vs μ directly determines the average $\langle a_q \rangle$ independent of that multiplicative factor.

Besides $F_q^{h,v}$ and $(\ln F_q^{h})^{v}$, one can also consider the $F_q^{v,h}$ moments, which is vertically analyzed, horizontally averaged, i.e.,

$$F_q^{v,h} \equiv \frac{1}{M}\sum_{j=1}^{M}\frac{\langle n_j(n_j-1)\cdots(n_j-q+1)\rangle}{\langle n_j \rangle^q} \tag{3.2}$$

and the counterpart of (3.1), viz,

$$(\ln F_q^{v})^{h} \equiv \frac{1}{M}\sum_{j=1}^{M}\ln\left[\frac{\langle n_j(n_j-1)\cdots(n_j-q+1)\rangle}{\langle n_j \rangle^q}\right] . \tag{3.3}$$

Note that the average factorial products in (3.2) and (3.3) are normalized bin by bin, since, as is evident from Fig. 1, $\langle n_j \rangle$ varies within the window Y and therefore should

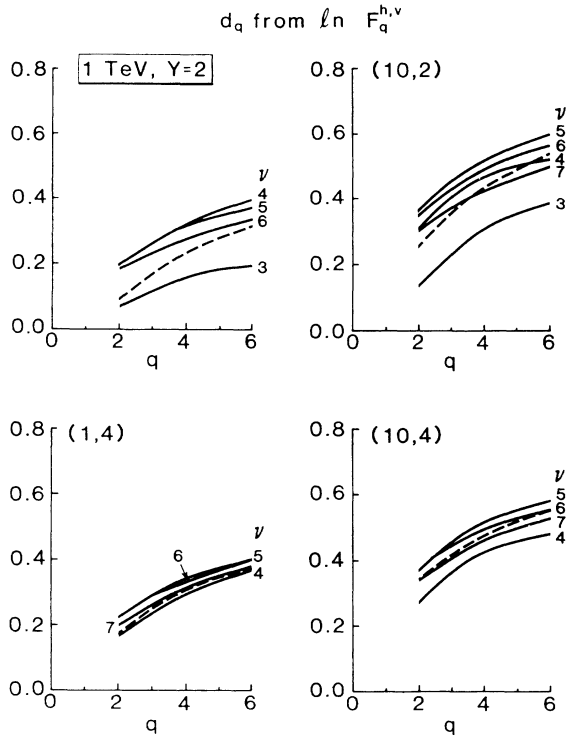

FIG. 4. Anomalous fractal dimensions d_q determined from $\ln F_q^{h,v}$ for various values of s, Y, and ν. The dashed line is for global average over all events regardless of ν.

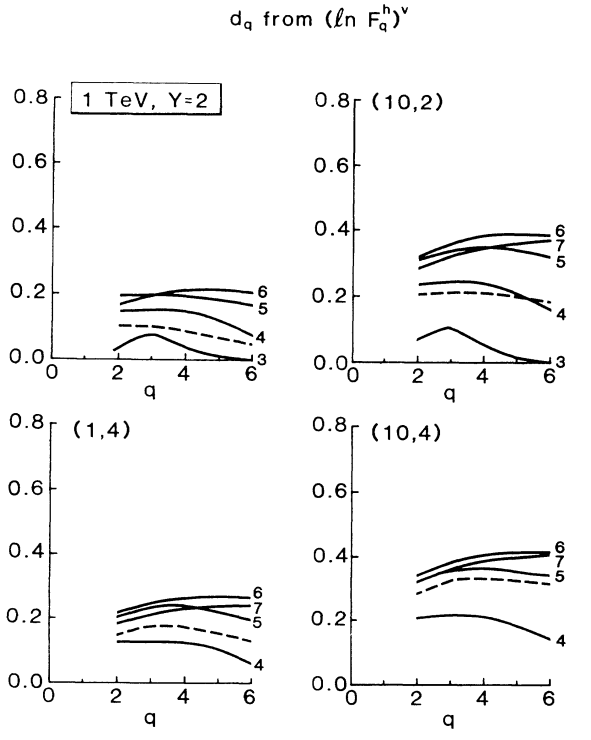

FIG. 5. Anomalous fractal dimensions d_q determined from $(\ln F_q^{h})^{v}$ for various values of s, Y and ν. The dashed line is for global average over all events regardless of ν.

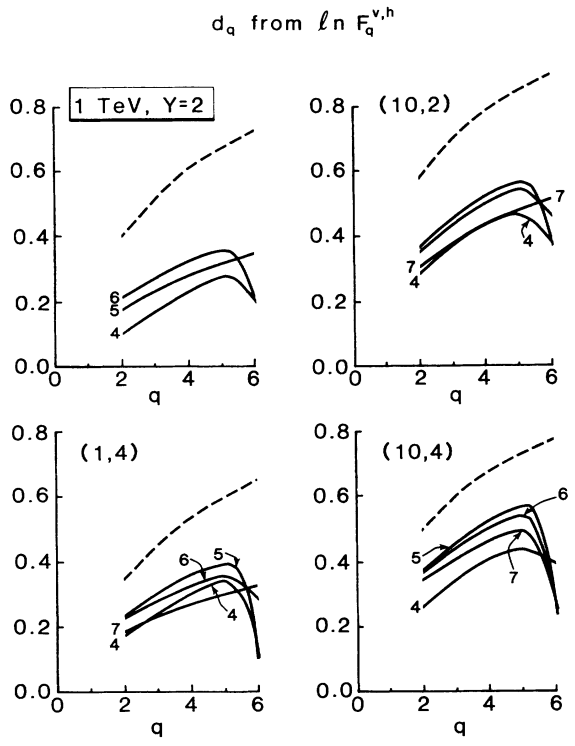

FIG. 6. Anomalous fractal dimensions d_q determined from $\ln F_q^{v,h}$ for various values of s, Y, and ν. The dashed line is for global average over all events regardless of ν.

not be approximated by $\langle N \rangle / M$ and taken outside the sum over j.

In view of the many combinations of variables in the sYN space where we study all four types of $\ln F_q$ vs μ for a range of q, we present only our final results in terms of the anomalous fractal dimension

$$d_q = \frac{a_q}{q-1} , \tag{3.4}$$

where a_q is determined from the $0 \le \mu \le 4$ interval in the log-log plots in each case. In Figs. 4–7 the results from our study of F_q are shown for $\sqrt{s} = 1$, 10 TeV, $Y = 2,4$, and a range of ν in each figure. The four figures show the values of d_q obtained from analyzing the four different averages of the factorial moments: $\ln F_q^{h,v}$, $(\ln F_q^h)^v$, $\ln F_q^{v,h}$, and $(\ln F_q^v)^h$, in that order. In all the graphs we have used dotted lines to show the results from averaging over all events without regards for the ν values. Note that in Figs. 6 and 7 the dotted lines are above all the solid lines, and therefore appear to contradict the notion that they represent the averages of the solid lines. That notion is, however, incorrect, because the average of a set of solid lines implies an average of the quotients in the large parentheses of (3.3), which is not equivalent to the quotient of the global averages over all events. No such problem appears in Figs. 4 and 5 since vertical averages are taken after the horizontal analysis is done, as is evident in (2.1) and (3.1), where only one $\langle \cdots \rangle$ appears in each of the equations.

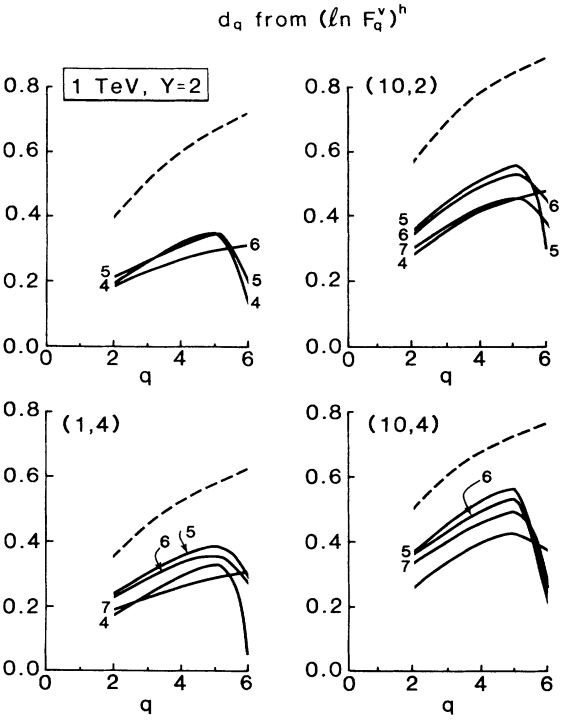

FIG. 7. Anomalous fractal dimensions d_q determined from $(\ln F_q^v)^h$ for various values of s, Y, and ν. The dashed line is for global average over all events regardless of ν.

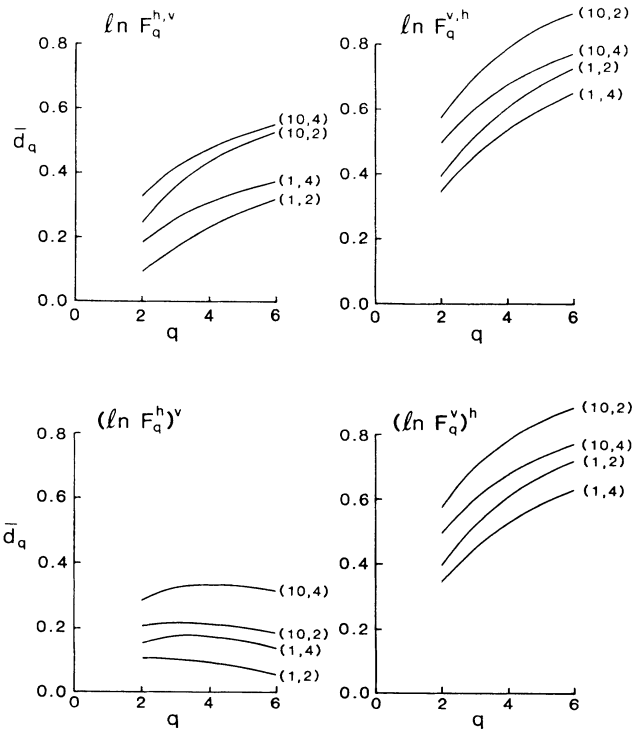

FIG. 8. Collection of all the global averages represented by the dashed lines in Figs. 4–7.

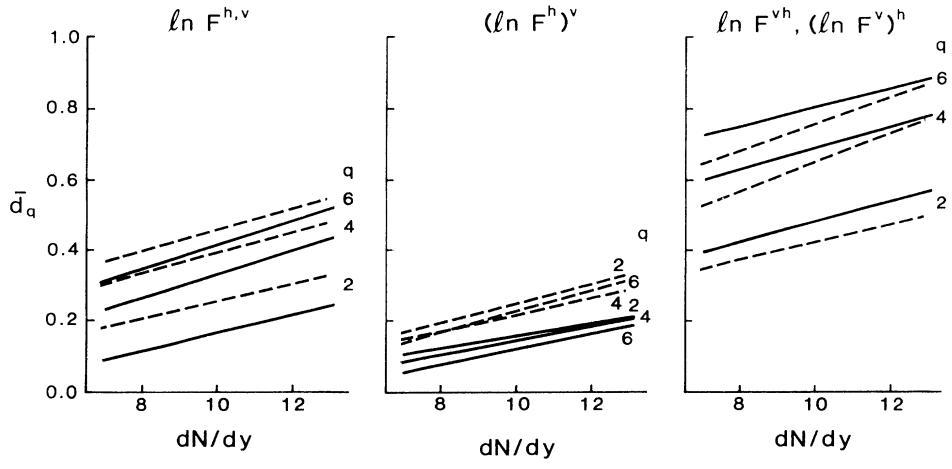

FIG. 9. Global averages $\bar{d}_q$ vs dN/dy for $q=2,4,6$. Solid lines are for $Y=2$ and the dashed lines for $Y=4$.

Upon examining the four sets of figures in Figs. 4–7, we find no similarity except between Figs. 6 and 7. In each figure the value of d_q depends on s, Y, and ν. The dependence on q in Fig. 5 is milder than in any of the other three figures. In each figure the q dependence of d_q is roughly not dependent on sYN, although the magnitudes of d_q do. Since no general characterization of the ν dependences can be made, we shall pursue that aspect of the complication no more in this section. Focusing on the averages over all events represented by the dashed lines in these figures, we can first of all collect the 16 curves, denote them by $\bar{d}_q$ and plot them in Fig. 8. Again, within each type of averaged moments considered, there is more dependence on s and Y than on the way they change with q.

The sY dependence can be collectively described in terms of either dN/dy or $\langle N\rangle$. In Fig. 9 we show how $\bar{d}_q$ depends on dN/dy for $q=2$, 4, and 6. The solid lines are for $Y=2$ and the dashed lines are for $Y=4$. Straight lines are plotted between the end points to guide the eye. The most striking feature of this figure is that $\bar{d}_q$ increases with dN/dy, contrary to the trend that Buschbeck and Lipa [11] found in other collisions. The slopes of $\bar{d}_q$ vs dN/dy are all very similar in all figures in Fig. 9.

In the case of $(\ln F_q^h)^v$, there is very little dependence on q. Thus, we may use $\bar{d}$ to denote the range of $\bar{d}_q$ values and examine its dependence on $\langle N\rangle$. Our simulation yields the values of $\langle N\rangle$ for the four cases of $(\sqrt{s}, Y)$ as follows: 14 (1,2), 27.5 (1,4), 26.2 (10,2), 51.4 (10,4). In Fig. 10 we have plotted $\bar{d}$ vs $\log\langle N\rangle$, exhibiting an approximate linear rise, irrespective of s and Y individually.

In summary we conclude that we have studied the factorial moments with different definitions and different averages. The intermittency indices have complicated dependences on sYN and q. The simplest features that we can extract are the linear rise of $\bar{d}_q$ with dN/dy in all cases, and the logarithmic increase of the average $\bar{d}$ of

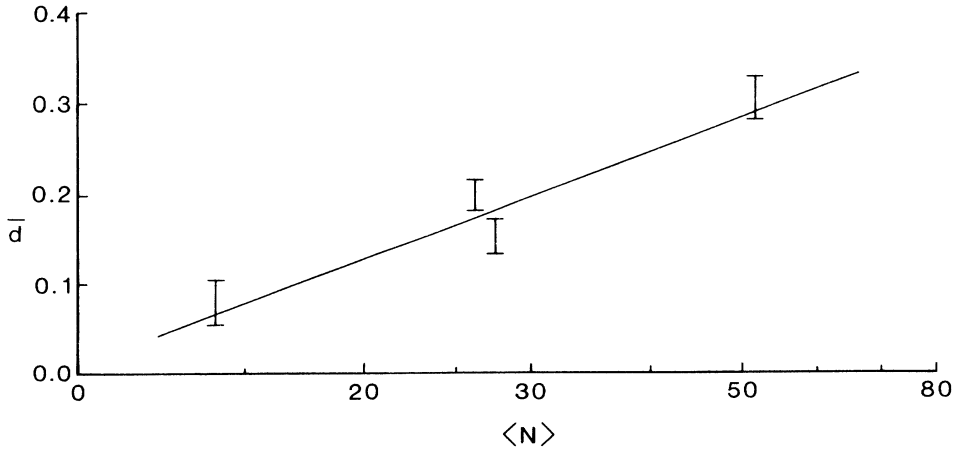

FIG. 10. Anomalous fractal dimension from $(\ln F_q^h)^v$ averaged over all events (the dashed lines in Fig. 5) vs average multiplicity within Y.

$(\ln F^h)^\nu$ with $\langle N \rangle$. If we regard these features as universal characteristics of e^+e^- annihilation, a property that requires experimental verification, then we may use them to compare with similar quantities in other collision processes. The point we try to make here is that it is meaningless to compare the intermittency index of e^+e^- annihilation determined at particular values of s, Y, and N with the indices of other collision types at other values of sYN.

IV. THE G MOMENTS

In studying the multifractual structure of multiplicity fluctuations, we have found that the G moments form a convenient starting point of the analysis [4,5]. In Ref. [4], vertical analysis was proposed, but the method has not been applied to any model or data analysis. Horizontal analysis was considered in Ref. [5] for the ϕ^3 and gluon models, and the method has been applied to the analysis of the e^+e^- annihilation data [12], the μp production data [13], as well as hadronic collision data [14,15]. In the following we shall continue to consider the horizontal analysis of the fluctuations, which is then averaged vertically.

For a quick summary of the method, we define for each event [5]

$$G_q = \sum_{j=1}^{M}{}' p_j^q , \tag{4.1}$$

where $p_j = n_j/N$, which is the fraction of number of particles in the jth bin, and the summation is over nonempty bins only. The order q can be any real number, positive or negative. If there is multifractal structure, then G_q should have the power-law behavior

$$G_q \propto \delta^{\tau(q)} . \tag{4.2}$$

From $\tau(q)$ we can determine

$$\alpha_q = \frac{d}{dq}\tau(q) . \tag{4.3}$$

$$f(\alpha) = q\alpha_q - \tau(q) . \tag{4.4}$$

While this can be done for each event, it is preferable, for the sake of statistics if not for other reasons, to perform a vertical averaging over G_q or $\ln G_q$ before calculating α and $f(\alpha)$.

To explore the universality of the G moments, the dependences on μ and ν have been considered in Ref. [16]. It was found that, under certain assumptions about a multiplicity splitting function, the G moments satisfy the relation

$$\ln G_q(\mu,\nu) = \Gamma_q(\mu-\nu) - \Gamma_q(-\nu) , \tag{4.5}$$

where $\Gamma_q(\xi)$ is a universal scaling function of one variable ξ. This property of universality has been verified by the UA1 data [17]. We have calculated $\ln G_q(\mu,\nu)$ in JETSET for e^+e^- annihilation and found that (4.5) is not satisfied. Thus, the universality found in the UA1 data is process dependent. For e^+e^- annihilation, it therefore remains for us to search for other aspects of universality.

How does the sYN syndrome manifest itself in the G moments and therefore in the $f(\alpha)$ spectrum? It has all the complexities of the F moments, plus more arising from the negative q moments, which are worse. For fixed s and Y, we have attempted to find universal properties of $G_q(\mu,\nu)$ along the lines of finite-size scaling and multifractal scaling [18,19] on the basis that the complicated μ and ν dependences in our problem are rooted in the realities of particle physics, where the number of particles produced is finite and where there can be no scaling property even at infinite resolution. Unfortunately, our attempt failed in uncovering any hidden universality by rescaling the variables.

On the $f(\alpha)$ spectrum we present first, as an illustration, the result of our multifractal analysis on $\langle \ln G_q \rangle$ for a specific set of sYN. We first vertically average $\ln G_q$, then find the $\tau(q)$ using (4.2), and finally determine $f(\alpha)$ using (4.3) and (4.4). At 1 TeV and $Y=2$ the results for $\nu=3,\ldots,6$ are shown in Fig. 11. All curves have negative curvatures with $f(\alpha)\leq\alpha$. While the curves show the proper behaviors appropriate for $f(\alpha)$ spectra [4,20,21], their relationship with one another shows no universality, even though there is some regularity in that the curves broaden with increasing ν.

We now ask whether the event structure of our simulation should be filtered in some way in order to reveal more clearly the properties of self-similarity in the G moments. In the remainder of this section we discuss the rationale and procedure for the selection of events, whose G moments exhibit cleaner power-law behavior. From the modified averages of those G moments we can then identify universality in the next section. All the averages considered in the rest of this paper will be on $\ln G_q$, not on G_q themselves.

If the averages of $\ln G_q$ are plotted against μ, the negative moments typically rise rapidly and then saturate in such a way that there is no extensive linear range in which one can comfortably claim self-similarity as expressed by (4.2). Many such graphs have been shown by Sugano [12] in his analysis of the High Resolution Spectrometer data on e^+e^- annihilation. An example of such behavior is shown by the dashed lines in Fig. 12 generated by our simulation. While the line for the positive mo-

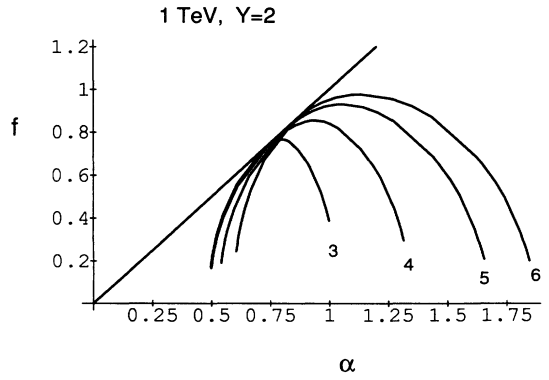

FIG. 11. Multifractal spectrum $f(\alpha)$ determined from $\langle \ln G_q \rangle$ for various values of ν at $\sqrt{s}=1$ TeV and $Y=2$.

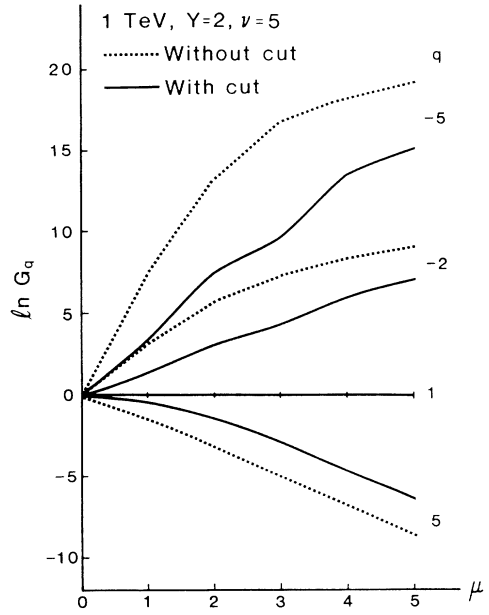

FIG. 12. $\ln G_q$ determined by averaging over only those events having $\nu=5$ (more precisely $26\le N\le 38$) at $(\sqrt{s},Y)=(1,2)$. Dashed lines are for uncut events; solid lines are for events with cuts specified by Eqs. (4.6) and (4.7).

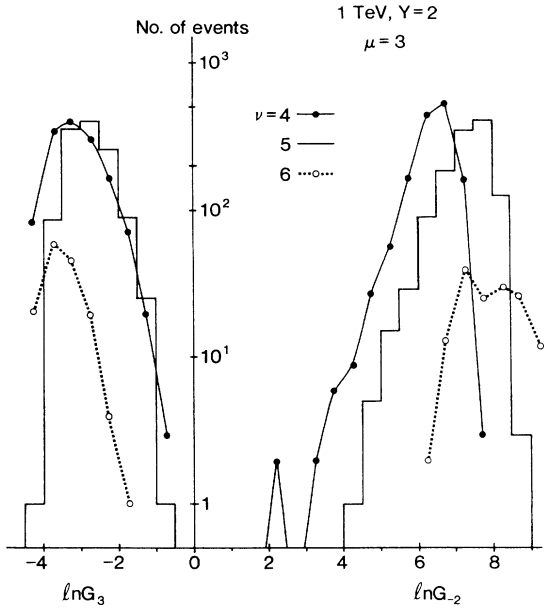

FIG. 13. Distribution of events in $\ln G_3$ and $\ln G_{-2}$ for $\mu=3$ and $\nu=4,5,6$ at $(\sqrt{s},Y)=(1,2)$.

ment is quite straight, it is hard to assign unique slopes $\tau(q)$ to the negative moments because of the curvatures. The $f(\alpha)$ spectra in Fig. 11 have been calculated from the initial slopes $\tau(q)$ determined from the $\mu=1-2$ interval in the plots such as the dashed lines in Fig. 12.

It is not hard to find the source of the problem. Unlike fractorial moments, the multifractal analysis probes the properties of both the peaks with $q>1$ moments, and of the dips with the $q<1$ moments. For example, the $q=0$ moment measures the number of nonempty bins: consequently, $f(\alpha_0)$ is the fractal dimension. The large negative G moments are particularly sensitive to the dips. From (4.1) we see that $p_j=0$ is not included in the sum because it is an empty bin, but if there is a bin with only one particle in it, then $p_j=1/N$ and its contribution to G_q is N^{-q}, which can become very large when q is a large negative number. Moreover, that contribution has no dependence on M upon further bin splitting, since only one sub-bin can contain that particle, contributing the same $1/N$ value to p_j, while all other empty sub-bins, by definition, do not contribute to G_q. It is the events of this type that contribute to the saturation effect associated with the dashed lines in Fig. 12, and is a problem special to particle physics.

One way to treat this problem is to exclude such events from our analysis by making cuts on the sample of events to be analyzed [22]. If a subsample of events can exhibit self-similarity for both positive and negative moments, the problem encountered above can then be avoided. In order to see how sensible cuts can be made, we show in Fig. 13 an illustration of the distribution of $\ln G_q$ for $q=-2$ and $+3$, remembering that every event has a specific value of $G_q(\mu,\nu)$. The distribution in Fig. 13 is for $\sqrt{s}=1$, TeV, $Y=2$, $\mu=3$, $\nu=4,5,6$. Out of a total 10 K events for this simulation, there are 1395 events for $\nu=4$ ($14\le N\le 18$), 1204 events for $\nu=5$ ($25\le N\le 38$) and 147 events for $\nu=6$ ($51\le N\le 76$). The average values $\langle \ln G_q\rangle$ are 6.4, 7.3, 7.9, respectively, for $q=-2$, and -2.6, -2.8, -3.0, respectively, for $q=+3$. It is not crucial which μ and which positive and negative q values one considered, but it is important to recognize that the events whose $|\ln G_q|$ in Fig. 13 are less than $|\langle \ln G_q\rangle|$ for both $q=+3$ and -2 must have high peaks without nonempty deep dips. The cut on G_3 favors peaks, while the cut on G_{-2} suppresses nonempty deep dips. Such events should therefore not contribute to the saturation effect seen in the dashed lines in Fig. 12. To control the selection criteria, let us introduce a parameter Z in defining a sample $S(Z)$ of events, in which $\ln G_q$ satisfies the bounds:

$$\ln G_3 \ge Z\langle \ln G_3\rangle , \tag{4.6a}$$

$$\ln G_{-2} \le Z\langle \ln G_{-2}\rangle , \tag{4.6b}$$

at $\mu=3$. There is a distinct sample $S(Z)$ for each sYN. Within each sample we can calculate the averages $\langle \ln G_q\rangle_Z$ for all q and μ. We lower the value of Z until $\langle \ln G_q\rangle_Z$ vs μ exhibits linear behavior over a wide range of μ for all q values. We have found that behavior at

$$Z=0.8 \tag{4.7}$$

as shown by the solid lines in Fig. 12. Because of the reduced number of events in these samples with the cut of (4.6), the lines are not smooth. However, it is clear that the behaviors in the range $0\le\mu\le 4$ can well be approximated by straight lines joining the points at $\mu=0$ and 4. For larger Z we lose linearity; for smaller Z there are too

few events to make meaningful plots. The parameter Z plays the same role as $p_{T_{\text{cut}}}$ in jet analysis in high-p_T experiments, where $p_{T_{\text{cut}}}$ should be large enough to reveal jet structure, but low enough to provide enough statistics.

We have here described the procedure for making cuts in the $\ln G_q$ distribution to enhance the self-similar behavior of the G moments. It should be emphasized that $q=-2$ and $+3$ have no preeminent attributes to qualify for use in the definition of cuts in (4.6). However, we know that $f(\alpha)$ peaks at $q=0$ and is equal to α at $q=1$ [4,5], so it is sensible to choose $q=-2$ and $+3$ on the two sides of the $0\le q\le 1$ region to serve as guideposts for our cut procedure. Similarly, we have chosen $\mu=3$ for the application of (4.6), since it is on the high side of the range $0\le\mu\le 4$ where we can reasonably expect linear behaviors to emerge in $\langle \ln G_q \rangle_Z$ vs μ, as is evident in Fig. 12. The content of the multifractal structure should be independent of these choices.

V. UNIVERSALITY IN MULTIFRACTAL STRUCTURE

We have seen in the preceding section how cuts in $\ln G_q$ result in event samples $S(Z)$ that possess clear self-similarity in multiplicity fluctuations. We now perform multifractal analysis of those samples and investigate the possible existence of universality.

With Z set at 0.8 we have run for the four cases of $(\sqrt{s}, Y)$ the following number of events: 180 K (1,2), 180 K (10,2), 65 K (1,4), and 65 K (10,4). The plots of $\langle \ln G_q \rangle_Z$ vs μ at (1,2) and $\nu=5$ are shown in Fig. 14 for a range of q; three of them are already included in Fig. 12. The number of events in this sample is 4332 out of the total of 180 K. For $-2\le q\le 1$ we have made runs with small incremental differences in q so that we can determine $d\tau(q)/dq$ with accuracy in that crucial range where $f(\alpha)$ turns from positive to negative slope in α. The slopes $\tau(q)$ are determined by the straight-line approximation between $\mu=0$ and 4.

The results on $f(\alpha)$ from the analysis using (4.3) and (4.4) are shown in Figs. 15 and 16 for the four cases of s and Y, in each of which a range of ν values with enough events are considered. Evidently, the $f(\alpha)$ spectra all have similar shapes. They all satisfy $f(\alpha)\le\alpha$, and $d^2f/d\alpha^2<0$; they broaden uniformly as ν increases. Visually they are symmetrical, although in reality they are not, as we shall see later. Obviously, these curves have more regularity than the ones shown in Fig. 11. Moreover, the similarity among the four sY cases is striking.

For given s and Y, the $f(\alpha)$ curves move up and become wider for increasing ν. The first is easier to understand. At high N the number of nonempty bins increases, so the fractal dimension, which is $f(\alpha)$ at the peak [4,20], also increases. Consequently, $f(\alpha)$ moves up and to the right. The upward movement of the peak will saturate at $f(\alpha_0)=1$, which is the topological dimension. Why the curves widen is harder to explain. Roughly speaking, a wider $f(\alpha)$ corresponds to more fluctuation. At low N, there are many empty bins, especially when M is large. They are not counted in the G moments, but the reduced number of nonempty bins also reduces the degree of multiplicity fluctuations, particularly since the sample $S(Z)$ with cuts suppresses the inclusion of events with low bin multiplicities. At high N, there are more bins with larger variety of bin multiplicites, thus contributing to more

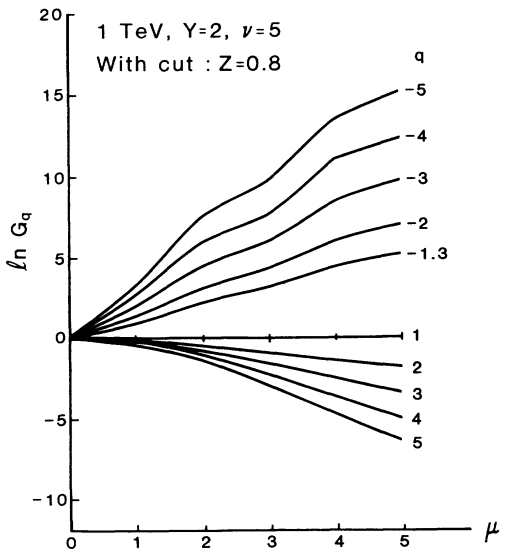

FIG. 14. log-log plot of G moments for $\ln G_q$ averaged over events in the cut sample $S(Z)$ for $\nu=5$ at $(\sqrt{s}, Y)=(1.2)$.

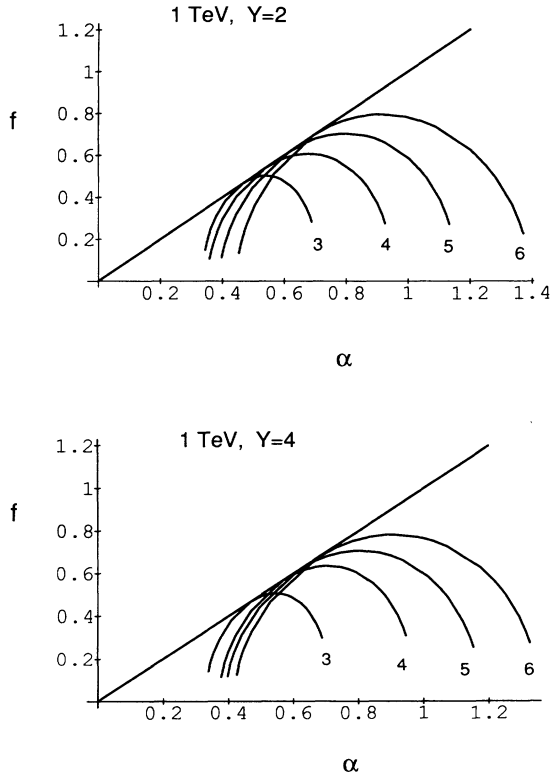

FIG. 15. Multifractal spectra $f(\alpha)$ determined from $\langle \ln G_q \rangle_Z$ for various values of ν at $(\sqrt{s}, Y)=(1,2)$ and $(1,4)$.

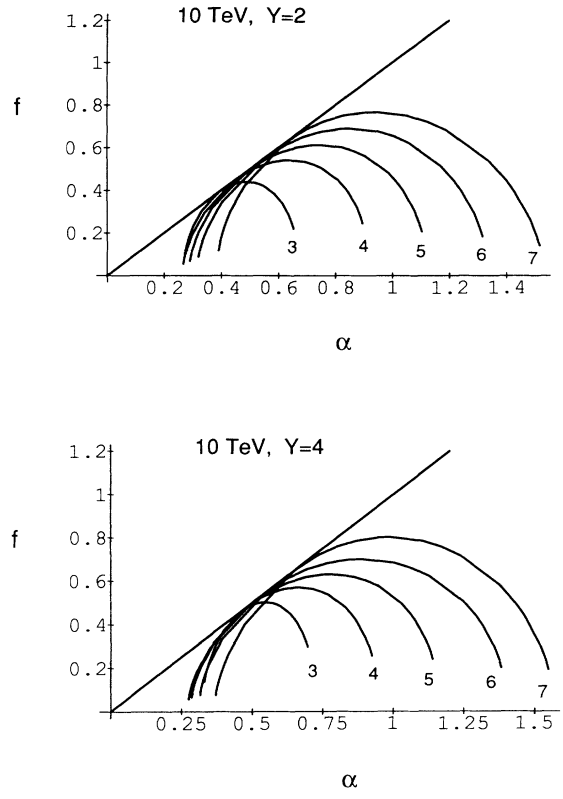

FIG. 16. Multifractal spectra $f(\alpha)$ determined from $\langle \ln G_q \rangle_Z$ for various values of ν at $(\sqrt{s}, Y)=(10,2)$ and $(10,4)$.

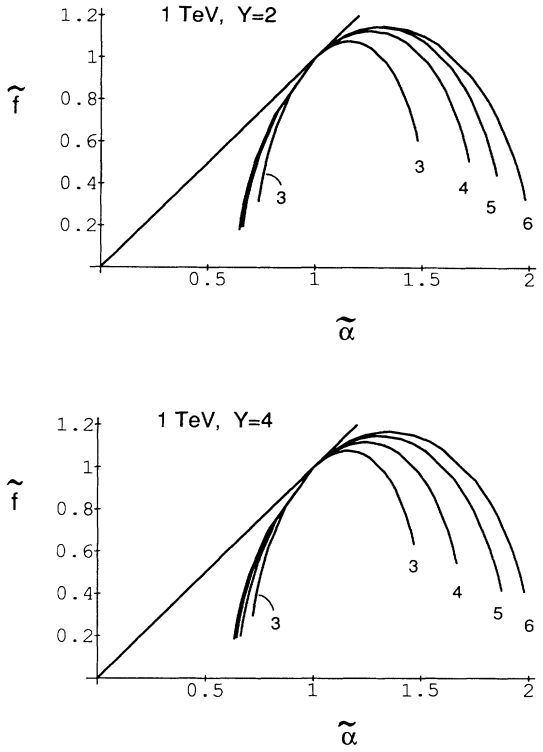

FIG. 17. Rescaled multifractal spectra $\tilde{f}(\tilde{\alpha})$ for the parameters of Fig. 15.

fluctuation.

To sharpen the relationship among the various ν curves, let us rescale those curves in the following way. First, recall that $f(\alpha)=\alpha$ is always true at $q=1$, as can easily be seen from (4.4) and the fact that $\tau(1)=0$, since $G_1=1$. Since, at that point, α_1 is the information dimension [23,24], i.e.,

$$\alpha_1=\lim_{\delta\to 0}\left[\sum_{j=1}^{M}{}' p_j \ln p_j\right] \Big/ \ln\delta \ , \tag{5.1}$$

let us refer to that point in the $f(\alpha)$ curve as the information point. Now we define the rescaled $\tilde{\alpha}$ and $\tilde{f}$:

$$\tilde{\alpha}=\alpha/\alpha_1 \ , \tag{5.2a}$$

$$\tilde{f}=f/f(\alpha_1)=f/\alpha_1 \ . \tag{5.2b}$$

If we do this for all ν curves, then all $\tilde{f}(\tilde{\alpha})$ curves coincide at $\tilde{\alpha}=\tilde{f}(\tilde{\alpha})=1$. Figures 17 and 18 show the results of this rescaling on the curves that are in Figs. 15 and 16, respectively. Remarkably, except for $\nu=3$, all the $\tilde{f}(\tilde{\alpha})$ curves coincide for $\tilde{\alpha}\le 1$. This is a form of universality that unifies the multifractal structure for $q\ge 1$. Even for $\nu=3$, the breaking of universality is not severe, a property that becomes all the more noteworthy when one recognizes the wide range of N values (from 8 to 128 in Y) being analyzed in, say, 16 bins ($\mu=4$). Above the information point where $\tilde{\alpha}>1$ ($q<1$), the universality fails to hold true. This may be understandable from the point of view that the cut sample $S(Z)$ is designed to enrich the

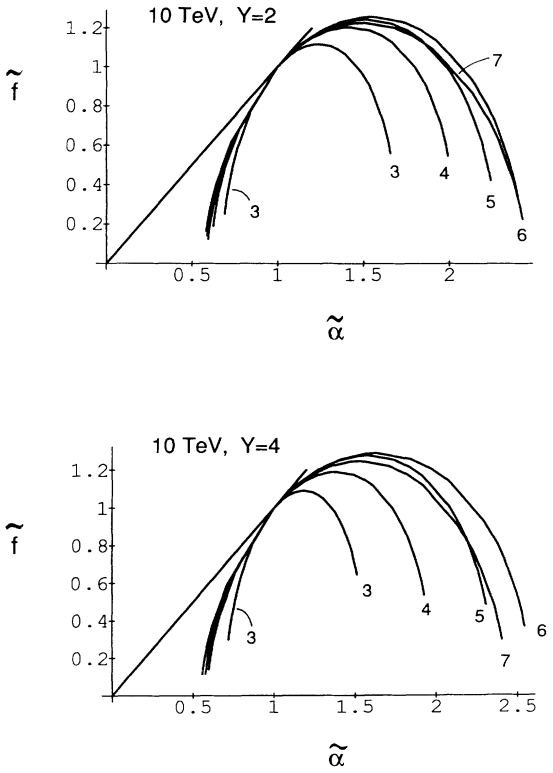

FIG. 18. Rescaled multifractal spectra $\tilde{f}(\tilde{\alpha})$ for the parameters of Fig. 16.

proportion of events with peaks at the expense of events with deep dips, so we would be too optimistic to expect simplicity to arise also from the $q<1$ moments, which characterize the dips. Thus, if we limit our focus to the peak structure, as intermittency does, then we have found the universality in the $\tilde{f}(\tilde{\alpha})$ curves.

Having unified the various ν curves, we now examine the sY dependence. In Fig. 19 we combine all four graphs in Figs. 17 and 18, excluding the $\nu=3$ curves. It is evident that all 15 $\tilde{f}$ curves overlap very well in the $\tilde{\alpha}<1$ region. We have thus found a remarkable sYN universality, when the multifractal spectrum is expressed in $\tilde{f}(\tilde{\alpha})$. It is this $\tilde{f}(\tilde{\alpha})$ spectrum that one may use to represent e^+e^- annihilation, when comparisons are to be made with other collision processes.

Because of the Z cut on the events, the normalization of $\langle \ln G_q \rangle_Z$ has, of course, been reduced from that of $\langle \ln G_q \rangle$ without the cut. As a consequence, the normalizations of $\tau(q)$, α, and f are all reduced accordingly, and depend on Z. However, the rescaled $\tilde{\alpha}$ and $\tilde{f}$ are independent of Z on account of (5.2). Thus, the universality of $\tilde{f}(\tilde{\alpha})$ in Figs. 17–19 is a property that should be independent of the cut.

It is of interest to present the results on the global average $\langle \ln G_q \rangle_{\text{all } N}$, where the average is performed over all events in sY, regardless of N. Of course, without cuts in $\ln G_q$, the plots of $\langle \ln G_q \rangle_{\text{all } N}$ vs μ have saturation effects for negative q, just like the dashed lines in Fig. 12 (which is specifically for $\nu=5$). If one, nevertheless, extracts the slopes $\tau(q)$ from the $\mu=1-2$ interval and computes $f(\alpha)$, the result is as shown in Fig. 20 for the four sY cases. There is nothing about those curves that we may identify as universal.

We have performed a cut procedure on $\langle \ln G_q \rangle_{\text{all } N}$ with $Z=0.8$. Here the quality of linearity is not as good as those for the fixed-N analysis. In principle, one may choose to vary Z to obtain better linear behavior. However, it is unclear whether it is justified to consider different Z values between the fixed-multiplicity analysis and the "all" analysis. Following the same procedure as before, we have calculated $\tilde{f}(\tilde{\alpha})$ for the global averages. The result is shown in Fig. 21. Evidently, the $\tilde{\alpha}<1$ region is now approximately universal. Moreover, the $\tilde{f}(\tilde{\alpha})$ curves in Fig. 21 can be embedded among those in Fig. 19. Thus, we have the final satisfactory result that $\tilde{f}(\tilde{\alpha})$ for $\tilde{\alpha}<1$ is essentially the same for all sYN as well as for the global averages at all sY.

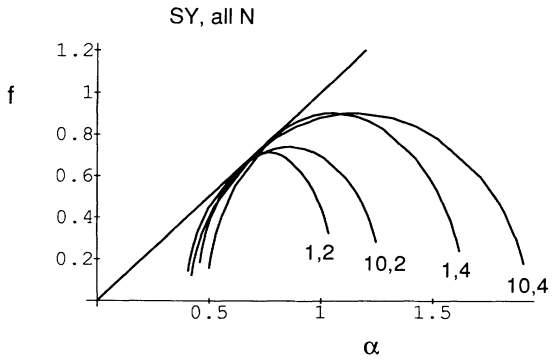

FIG. 20. Multifractal spectrum $f(\alpha)$ determined from $\langle \ln G_q \rangle_{\text{all } N}$ for various combinations of $(\sqrt{s}, Y)$.

We have investigated the possibility of a simple relationship between intermittency and multifractality. Theoretically, we have found none without making invalid approximations about the factorial moments. Empirically, it is obviously hard to identify any simple relationship between the (1,2) graph of Fig. 5 and either Fig. 11 or the (1,2) graph of Fig. 15. Roughly, one may expect $\bar{\alpha}_1 \approx 1-\bar{d}$ if the multifractal spectrum is narrow enough to resemble a monofractal. But Figs. 19 and 21 tell us that the multiplicity fluctuation is far from being a monofractal. Judging from the results described in Sec. III and in this section, we conclude that the multifractal structure contains universal features that are difficult to uncover in intermittency analysis.

VI. CONCLUSION

Using JETSET to simulate events in e^+e^- annihilation, we have exhaustively studied the properties of multiplicity fluctuations in the framework of intermittency and multifractality. The justification for this investigation is two-fold. On the one hand, we have opened up new terri-

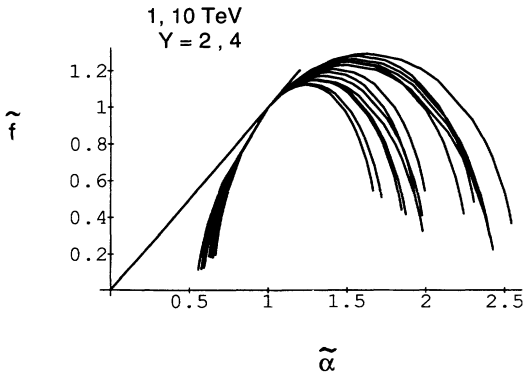

FIG. 19. Superimposition of all $\tilde{f}(\tilde{\alpha})$ curves in Figs. 15–18 excluding $\nu=3$.

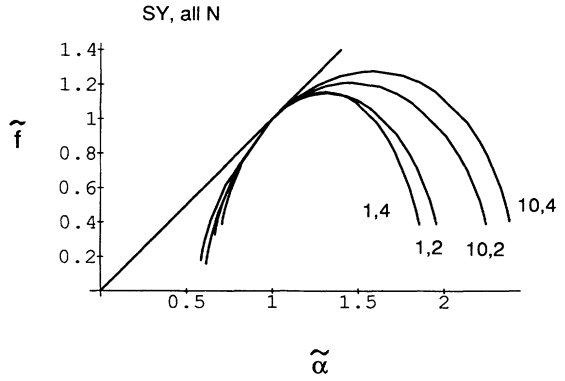

FIG. 21. Rescaled multifractal spectrum $\tilde{f}(\tilde{\alpha})$ of the curves determined from $\langle \ln G_q \rangle_Z$ based on all events for various combinations of $(\sqrt{s}, Y)$.

tories in which detailed properties of particle production are not known experimentally, and which provide further in-depth tests of the Lund parton shower model, or any other dynamical model. On the other hand, assuming that JETSET is faithful in its simulation of reality, we have found complications that were hitherto unsuspected; fortunately, some aspects of those complications can be organized into universal properties, which can be regarded as the basic characterization of the annihilation process.

Dependences on s and Y are obvious features that should be clarified. However, we have pushed further to inquire about the dependence on N, not just on $\langle N \rangle$. We can mention two reasons to support our advocacy for the study of the N dependence. The first is a logical extension of the advances made by intermittency: just as the investigation of multiplicity fluctuations in small rapidity bins reveal structure that is smeared out in large rapidity intervals, the N dependence reveals complications that are covered up in global averages. The second reason may not be so obvious in e^+e^- annihilation. But when intermittency and multifractal analyses are applied to hadronic and especially nuclear collisions, N becomes an essential variable that is related to impact parameter, which significantly affects the collision processes. The insight and universality discovered here for e^+e^- annihilation should provide the impetus to perform similar analyses on the hadronic and nuclear data.

To summarize our results, we have found that the intermittency properties have complex dependences on s, Y, and N, the sYN syndrome. Among the various averages of the factorial moments, only $(\ln F_q^h)^v$, when averaged over all N, shows some simplicity in that the anomalous fractal dimension $\bar{d}$ is roughly q independent, and increases linearly with $\ln\langle N \rangle$, regardless of s and Y. No universality can be established in the N dependence. The behavior of $\bar{d}$ is somewhat unexpected, and should be checked by experiments in whatever range of $\langle N \rangle$ is accessible.

In multifractal analysis we have found that the $f(\alpha)$ spectra for global averages have no universal features. They are not free from the sYN syndrome when the N dependence is explored. To enhance the multifractal signal due to peaks in the rapidity distribution, we have made cuts in $\ln G_q$, and found that the cut sample of events exhibit better quality self-similarity and systematic behavior in $f(\alpha)$. The rescaled $\tilde{f}(\tilde{\alpha})$ spectra possess universality that is free of the sYN syndrome in the region $\tilde{\alpha} < 1$. These are the universal properties that characterize e^+e^- annihilation, and may be used for comparison with similar characterizations of other collision processes. As we have emphasized, it is only when an observable is free of the sYN syndrome can such comparisons be meaningful. Fractal dimensions and other generalized indices have no fundamental significance, if they lack the virtue of universality.

We have been disappointed by one aspect to this investigation, and that is our failure to establish a clear and quantitative connection between intermittency and multifractality. We have hoped to formulate a dictionary that can translate between intermittency indices a_q and multifractal indices α. The sYN syndrome has made the task difficult, and the absence of universality in intermittency has rendered it unfeasible. However, what is learned from this investigation is that multifractal analysis offers a better chance of uncovering universal characterization of multiplicity fluctuations.

Note added in proof. Some aspects of the connection between the F_q and G_q moments are discussed by R. C. Hwa and J. C. Pan, Phys. Rev. D **45**, 1476 (1992).

ACKNOWLEDGMENTS

We are grateful to T. Sjostrand for providing us the Monte Carlo code and manual for JETSET 7.3, without which this work could not have been done. This work was supported in part by the U.S. Department of Energy under Grants Nos. DE-FG05-85ER-40200 and DE-FG06-85ER-40224.

[1] *Intermittency in High Energy Collisions,* Proceedings of the Sante Fe Workshop, Santa Fe, New Mexico, 1990, edited by F. Cooper, R. C. Hwa, and I. Sarcevic (World Scientific, Singapore, 1991); W. Kittel, in *Proceedings of the 20th International Symposium on Multiparticle Dynamics,* Gut Holmecke, Germany, 1990, edited by R. Baier and D. Wegener (World Scientific, Singapore, 1991).

[2] A. Bialas and R. Peschanski, Nucl. Phys. **B273**, 703 (1986).

[3] I. M. Dremin, Mod. Phys. Lett. A **3**, 1333 (1988); P. Lipa and B. Buschbeck, Phys. Lett. B **223**, 465 (1988); P. Carruthers, Int. J. Mod. Phys. A **4**, 5587 (1989).

[4] R. C. Hwa, Phys. Rev. D **41**, 1456 (1990).

[5] C. B. Chiu and R. C. Hwa, Phys. Rev. D **43**, 100 (1991); in *Intermittency in High Energy Collisions* [1].

[6] T. Sjostrand and M. Bengtsson, Comput. Phys. Commun. **43**, 367 (1987); T. Sjostrand, Int. J. Mod. Phys. A **3**, 751 (1988).

[7] T. Sjostrand, JETSET 7.3, 1990.

[8] TASSO Collaboration, W. Braunschweig *et al.*, Phys. Lett. B **231**, 548 (1989).

[9] DELPHI Collaboration, P. Abreu *et al.*, Phys. Lett. B **247**, 137 (1990).

[10] OPAL Collaboration, M. Z. Akrawy *et al.*, Phys. Lett. B **262**, 351 (1991).

[11] B. Buschbeck and P. Lipa, in *Intermittency in High Energy Collisions* [1].

[12] K. Sugano, in *Intermittency in High Energy Collisions* [1]; *Proceedings of the Workshop on Correlations and Multiparticle Production,* Marburg, Germany, 1990, edited by M. Plumer, S. Raha, and R. M. Weiner (World Scientific, Singapore, 1991), p. 240.

[13] N. Schmitz, in *Fluctuations and Fractal Structure,* Proceedings of the Ringberg Workshop, Ringberg Castle, Germany, 1991, edited by R. C. Hwa, W. Ochs, and N. Schmitz (World Scientific, Singapore, 1992).

[14] UA1 Collaboration, M. Markytan and H. Dibon, in *Intermittency in High Energy Collisons* [1].

[15] CDF Collaboration, F. Rimondi, in *Correlations and Multiparticle Production* [12], p. 276.

[16] W. Florkowski and R. C. Hwa, Phys. Rev. D **43**, 1548 (1991).
[17] H. Dibon and M. Markytan, in *Proceedings of the 20th International Symposium on Multiparticle Dynamics* [1].
[18] L. P. Kadanoff, S. R. Nagel, L. Wu, and S. M. Zhou, Phys. Rev. A **39**, 6524 (1989).
[19] C. Tang, Santa Barbara Report No. NSF-ITP-89-118 (unpublished).
[20] J. Feder, *Fractals* (Plenum, New York, 1988).
[21] T. C. Halsey *et al.*, Phys. Rev. A **33**, 1141 (1986).
[22] R. C. Hwa, Phys. Rev. D **44**, 915 (1991).
[23] H. G. E. Hentschel and I. Procaccia, Physica D **8**, 435 (1983).
[24] R. C. Hwa, in *Quark Gluon Plasma,* edited by R. C. Hwa (World Scientific, Singapore, 1990).